

Cite this: *Chem. Commun.*, 2012, **48**, 10541–10543

www.rsc.org/chemcomm

Core–shell structured mesoporous silica as acid–base bifunctional catalyst with designated diffusion path for cascade reaction sequences†

Ping Li,^{ab} Chang-Yan Cao,^a Zhe Chen,^{ab} Hua Liu,^{ab} Yu Yu^{ab} and Wei-Guo Song^{*a}

Received 7th August 2012, Accepted 31st August 2012

DOI: 10.1039/c2cc35718f

A core–shell structured mesoporous silica nanosphere with antagonistic acid and basic sites spatially isolated and designated diffusion path was fabricated and served as an efficient acid–base bifunctional catalyst for one-pot cascade reaction sequences with excellent activity and selectivity.

The cascade reaction sequence is a fascinating subject in catalysis.^{1–3} A rationally designed cascade reaction sequence can simplify the synthetic route, reduce the amount of waste and lower the operation cost. The key for a successful cascade reaction sequence is the multifunctional catalyst. With a suitable multifunctional catalyst, multiple synthesis steps can proceed in one pot with high yield toward the target products.^{4–10}

For a multifunctional catalyst to work smoothly, different or even incompatible active sites, such as acidic sites and basic sites, must be spatially isolated so that they can coexist on one catalyst.¹¹ There are several strategies to do so.^{12–25} For example, Helms *et al.* used star polymers as supports to separate acid and basic groups.¹⁵ Kaneda *et al.* used two types of layered clays, Ti⁴⁺-exchanged montmorillonite and Mg–Al hydrotalcite, as bifunctional catalysts.¹⁶ Yang *et al.* fabricated functionalized delicate yolk-shell nanoreactors with basic sites at yolk and acid sites at shell.²⁵ These multifunctional catalysts showed various degrees of success in cascade reactions. However, tedious preparation procedures, deactivation of the catalysts and low selectivity toward the target products are still issues that need to be addressed.

In addition to the spatial isolation of active sites, a higher goal in catalyst design is to arrange the location of the active sites in a rational manner, so that the order of the reaction sequence, the order of the active site location and the direction of mass transportation on catalyst surface agree well with each other.

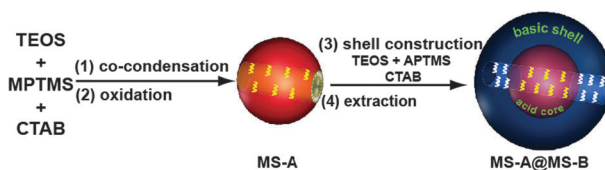
Herein, we report a core–shell structured mesoporous silica nanosphere as an acid–base bifunctional catalyst with the acid sites in the inner core and the basic group in the outer shell (MS-A@MS-B). With such a core–shell structure, acid and basic sites were spatially isolated. More importantly, the core–shell

structure offered a designated diffusion pathway for the reaction species. For two types of cascade reaction sequences, this catalyst showed superb activity and selectivity, *e.g.* nearly 100% conversion for the starting substrate and nearly 100% yield for the target product, while no intermediate species were detected.

The synthesis procedure for the core–shell structured catalyst is illustrated in Scheme 1. First, sulfonic acid groups modified mesoporous silica (MS-A) was prepared by co-condensation between tetraethyl orthosilicate (TEOS) and 3-mercaptopropyltrimethoxysilane (MPTMS) followed by the oxidation process. The resulting mesoporous silica core was then further coated with an amino group functionalized mesoporous silica shell using TEOS and 3-aminopropyltrimethoxysilane (APTMS) as mixed silica precursors. MS-A@MS-B was obtained after surfactant removal. For a control experiment, monofunctional catalysts with comparable active site concentration and the same core–shell structure, *i.e.* catalysts with only the amino group in the outer shell (MS@MS-B), or only the sulfonic acid group in the inner core (MS-A@MS) were prepared by similar methods.

The fabrication procedure was established with several considerations. Thiol groups were oxidized to sulfonic acid groups before the introduction of amino groups, otherwise amino groups would be destroyed by H₂O₂. In addition, the preferential functionalization of amino groups on the outer shell was successful as mesoporous channels of the core were occupied by CTAB during the shell coating process.²² With such a core–shell structure design, antagonistic acid and basic sites were spatially isolated. Moreover, by adjusting the ratios of different precursors in the synthesis mixture, the densities of the acid sites and basic sites, as well as the thickness of the core/shell in the catalyst, can be systematically tuned.

The TEM images (Fig. 1a, b) showed that the MS-A cores were relatively uniform nanospheres ranging from 50 to 70 nm in diameter with a disordered mesoporous structure. After the



Scheme 1 Synthesis procedure for acid–base bifunctional core–shell structured catalyst (yellow helix = –SO₃H, white helix = –NH₂).

^a Beijing National Laboratory for Molecular Sciences (BNLMS), Institute of Chemistry, Chinese Academy of Sciences, Beijing, 100190, P. R. China. E-mail: wsong@iccas.ac.cn; Fax: +86 10-62557908

^b Graduate University of Chinese Academy of Sciences, Beijing, 100049, P. R. China

† Electronic supplementary information (ESI) available: experimental details and characterization of catalyst. See DOI: 10.1039/c2cc35718f

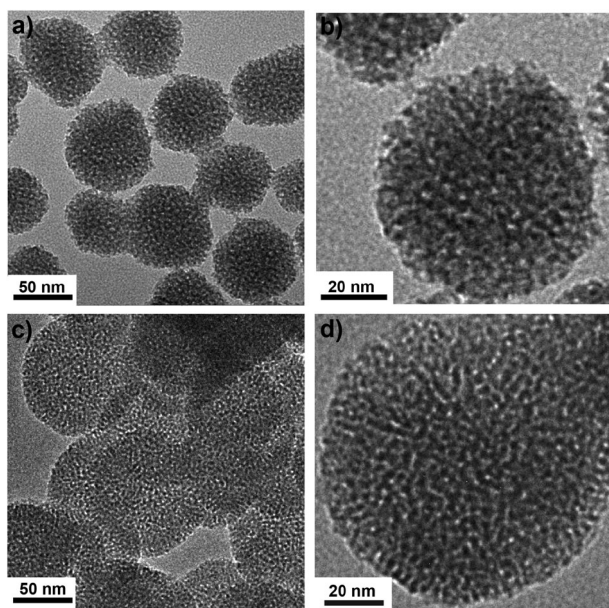


Fig. 1 (a) and (b) TEM images of MS-A; (c) and (d) TEM images MS-A@MS-B.

shell coating step, as shown in Fig. 1c and d, the sizes of the spheres increased to 80–110 nm. The low magnification TEM image in Fig. 1c exhibited subtle yet characteristic core-shell structure with slightly different grayness. The high magnification TEM image in Fig. 1d showed that the mesoporous channels of the outer shell were well-connected with those of the inner core, thus the mass diffusion pathway between the core and the shell was well-connected, which was critical for the catalytic applications.

From the nitrogen sorption measurement (Fig. S1a, ESI[†]), the MS-A@MS-B sample exhibited a typical type IV adsorption isotherm. A steep uptake in low relative pressure region ($0.2 < P/P_0 < 0.4$) was characteristic of capillary condensation, indicating the presence of a mesoporous structure. The BET surface area and pore volume were $950 \text{ m}^2 \text{ g}^{-1}$ and $0.62 \text{ cm}^3 \text{ g}^{-1}$, respectively. The inset in Fig. S1a (ESI[†]) showed a pore size distribution centered at 3.5 nm. The small-angle XRD pattern (Fig. S1b, ESI[†]) of MS-A@MS-B shows a large and broad diffraction peak that can be indexed to the (100) reflection.

The ^{29}Si solid-state NMR spectrum of the MS-A@MS-B sample is shown in Fig. S2a (ESI[†]). The presence of T^2 and T^3 peaks confirmed the strong covalent linkage between the organic groups and the silica surface. The ^{13}C solid-state NMR spectrum in Fig. S2b (ESI[†]) confirmed the successful grafting of the desired functional groups. In addition, XPS analysis (Fig. S3, ESI[†]) offered another evidence for the presence of acid sites in the core and basic sites in the outer shell. Elemental analysis showed MS-A@MS-B contained 0.35 mmol g^{-1} of sulfonic acid groups and 0.71 mmol g^{-1} of amino groups. Similar amounts of acid sites and basic sites were observed on the two control samples, MS-A@MS and MS@MS-B, respectively.

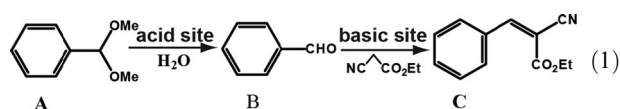


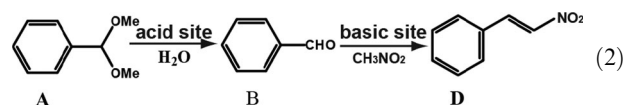
Table 1 One-pot deprotection-Knoevenagel cascade reaction sequence catalyzed by different catalysts^a

| Entry | Catalyst | Conv. of A (%) | Yield of B (%) | Yield of C (%) |
|------------------|------------------|----------------|----------------|----------------|
| 1 ^b | MS-A@MS-B | 79.5 | 0.5 | 79.0 |
| 2 | MS-A@MS-B | 100 | 0 | ≈100 |
| 3 | MS-A@MS | 20.0 | 20.0 | 0 |
| 4 | MS@MS-B | Trace | Trace | Trace |
| 5 | MS-A@MS-B/AP | 0 | 0 | 0 |
| 6 | MS-A@MS-B/PTSA | 18.0 | 18.0 | 0 |
| 7 | AP/PTSA | 0 | 0 | 0 |
| 8 ^{b,c} | Physical mixture | 71.4 | 14.4 | 57.0 |
| 9 ^c | Physical mixture | 93.7 | 15.7 | 78.0 |
| 10 | MS | 0 | 0 | 0 |

^a Reaction conditions: A (1 mmol), ethyl cyanoacetate (1.2 mmol), toluene (3 mL), catalyst (20 mg), reaction temperature = 80°C , reaction time = 0.5 h. Conversion and yield were determined using GC data. AP: 1-aminopropane, PTSA: *p*-toluene sulfonic acid. ^b Reaction time = 0.25 h. ^c Physical mixture composed of 20 mg of MS-A@MS and 20 mg of MS@MS-B.

The catalytic activity of MS-A@MS-B as an acid–base bifunctional catalyst was first tested in a one-pot tandem deprotection-Knoevenagel reaction (reaction (1)). The results were summarized in Table 1. MS-A@MS-B converted acetal to the desired product in almost quantitative yield after a reaction time of 0.5 h (Table 1, entry 2). In particular, during the reaction process, almost no intermediate species were detected (Table 1, entry 1 and 2, with different reaction time), showing high activity and excellent selectivity of the core-shell structured bifunctional catalyst. In sharp contrast, monofunctional catalysts with similar core-shell structures, MS@MS-B or MS-A@MS (Table 1, entries 3 and 4), didn't produce the desired target product, although MS-A@MS was able to catalyze the first step reaction to a small extent. Furthermore, the catalytic activity of the MS-A@MS-B sample was quenched when equivalent amounts of free acid or base was added (Table 1, entries 5 and 6), as these homogeneous molecules can deactivate the active sites.

In addition, a physical mixture of MS@MS-B and MS-A@MS with similar catalytic sites concentration was also tested (Table 1, entries 8 and 9). Both the activity and the selectivity of the reaction were significantly lower than those of the bifunctional MS-A@MS-B catalyst, indicating the synergistic effect of the core-shell structure. Note that using physical mixture of MS@MS-B and MS-A@MS led to significant amounts of intermediate species.



The catalytic performance of the MS-A@MS-B bifunctional catalyst was also evaluated in one-pot deacetalization-Henry reaction sequence (reaction (2)). MS-A@MS-B exhibited excellent performance (Table S1, entry 1, ESI[†]), whereas the control samples showed much lower abilities (Table S1, entries 2–8, ESI[†]).

The stability of the bifunctional catalytic system was also examined. The catalyst was recovered by centrifugation and directly reused in the next run. Results showed that the

core-shell structured catalyst could be recycled several times without a significant loss of catalytic performance. While the recycled physical mixture showed significant activity decay (see Table S2 and S3, ESI† for details), elemental analysis of the recovered core-shell structured catalyst showed the amount of sulfur and nitrogen were almost unchanged.

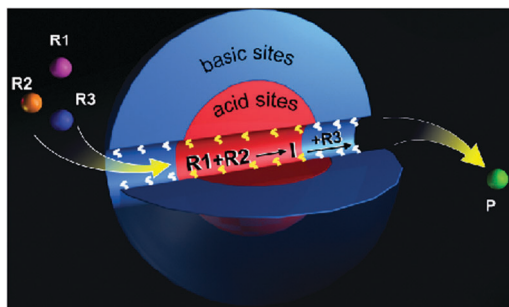


Fig. 2 Schematic reaction flow of the two-step cascade reaction sequences on the core-shell structured bifunctional catalyst MS-A@MS-B.

The catalytic performance of the MS-A@MS-B bifunctional catalyst was attributed to the nanoreactor features of the system. The core-shell structure not only spatially separated the two incompatible active sites, but also directed the reaction species to follow the desired diffusion pathway of the reaction sequence. As illustrated in Fig. 2, during the catalytic process, the reactants must pass through the outer shell to reach the inner core, where they were converted into the intermediate species (I) from the first reaction. To diffuse out of the catalyst sphere, the intermediate species must diffuse through the outer shell, where the basic sites converted it to the target product (P). Such a core-shell design with acid sites at the core and basic sites at the shell ensured that the intermediate species were converted before they left the catalyst, leading to excellent selectivity toward the target product during the whole catalytic reaction process (Table 1, entries 1 and 2; Table S1, ESI† entry 1). In comparison, in Yang *et al.*'s yolk-shell design with basic sites at the yolk and acid sites at the shell, a significant amount of intermediate product was observed.²⁵ When a physical mixture with comparable catalytic active sites concentration was used, a significant amount of intermediate species remained during the reaction (Table 1, entries 8 and 9; Table S1, ESI† entry 7). In addition, the confined effect as well as enrichment effect provided by the mesopores in the nanoreactor was also beneficial for fast reactions.

For future studies, several experimental aspects should be explored. More active sites can be added, *e.g.* noble metal nanoclusters may be added into either the inner core or the outer shell of the nanoreactor. The relative loading of basic and acid sites should be optimized to suit the relative reactivity of each step of the reaction sequence. More sequential reactions should also be designed to fully exploit this catalytic system.

In summary, we produced a core-shell structured acid-base bifunctional mesoporous silica nanosphere (MS-A@MS-B) with sulfonic acid group in the inner core and amino group in the outer shell. The core-shell structure allowed complete spatial separation of acid sites and basic sites. The rational designed spatial order of acid sites and basic sites led to excellent activity and selectivity in two types of reaction sequences, with nearly 100% conversion for the starting reactants and nearly 100% yield for the target products.

We thank the financial supports from the National Basic Research Program of China (2009CB930400), National Natural Science Foundation of China (NSFC 21121063), and the Chinese Academy of Sciences (KJXC2-YW-N41).

Notes and references

- 1 F.-X. Felpin and E. Fouquet, *ChemSusChem*, 2008, **1**, 718.
- 2 M. J. Climent, A. Corma and S. Iborra, *ChemSusChem*, 2009, **2**, 500.
- 3 M. J. Climent, A. Corma and S. Iborra, *Chem. Rev.*, 2010, **111**, 1072.
- 4 K. Motokura, M. Tada and Y. Iwasawa, *J. Am. Chem. Soc.*, 2007, **129**, 9540.
- 5 S. Shylesh, A. Wagner, A. Seifert, S. Ernst and W. R. Thiel, *Chem.–Eur. J.*, 2009, **15**, 7052.
- 6 A. El Kadib, K. Molvinger, M. Bousmina and D. Brunel, *J. Catal.*, 2010, **273**, 147.
- 7 A. Corma, T. Ródenas and M. J. Sabater, *Chem.–Eur. J.*, 2010, **16**, 254.
- 8 S. Shylesh and W. R. Thiel, *ChemCatChem*, 2011, **3**, 278.
- 9 F.-X. Zhu, W. Wang and H.-X. Li, *J. Am. Chem. Soc.*, 2011, **133**, 11632.
- 10 L. Xu, Y. Ren, H. Wu, Y. Liu, Z. Wang, Y. Zhang, J. Xu, H. Peng and P. Wu, *J. Mater. Chem.*, 2011, **21**, 10852.
- 11 B. Voit, *Angew. Chem., Int. Ed.*, 2006, **45**, 4238.
- 12 B. J. Cohen, M. A. Kraus and A. Patchornik, *J. Am. Chem. Soc.*, 1981, **103**, 7620.
- 13 F. Gelman, J. Blum and D. Avnir, *J. Am. Chem. Soc.*, 2000, **122**, 11999.
- 14 F. Gelman, J. Blum and D. Avnir, *Angew. Chem., Int. Ed.*, 2001, **40**, 3647.
- 15 B. Helms, S. J. Guillaudeu, Y. Xie, M. McMurdo, C. J. Hawker and J. M. J. Frechet, *Angew. Chem., Int. Ed.*, 2005, **44**, 6384.
- 16 K. Motokura, N. Fujita, K. Mori, T. Mizugaki, K. Ebitani and K. Kaneda, *J. Am. Chem. Soc.*, 2005, **127**, 9674.
- 17 N. T. S. Phan, C. S. Gill, J. V. Nguyen, Z. J. Zhang and C. W. Jones, *Angew. Chem., Int. Ed.*, 2006, **45**, 2209.
- 18 R. Abu-Reziq, D. Wang, M. Post and H. Alper, *Chem. Mater.*, 2008, **20**, 2544.
- 19 Y. L. Huang, B. G. Trewyn, H. T. Chen and V. S. Y. Lin, *New J. Chem.*, 2008, **32**, 1311.
- 20 A. Takagaki, M. Ohara, S. Nishimura and K. Ebitani, *Chem. Commun.*, 2009, 6276.
- 21 S. Shylesh, A. Wagerer, A. Seifert, S. Ernst and W. R. Thiel, *Angew. Chem., Int. Ed.*, 2010, **49**, 184.
- 22 Y. Huang, S. Xu and V. S. Y. Lin, *Angew. Chem., Int. Ed.*, 2011, **50**, 661.
- 23 N. R. Shiju, A. H. Alberts, S. Khalid, D. R. Brown and G. Rothenberg, *Angew. Chem., Int. Ed.*, 2011, **50**, 9615.
- 24 M. Sasidharan, S. Fujita, M. Ohashi, Y. Goto, K. Nakashima and S. Inagaki, *Chem. Commun.*, 2011, **47**, 10422.
- 25 Y. Yang, X. Liu, X. Li, J. Zhao, S. Bai, J. Liu and Q. Yang, *Angew. Chem., Int. Ed.*, 2012, **51**, 9164.